Jianjun Wang*, Xiaofang Shi, Lizhong Chang, Haijun Wang and Lipeng Meng

Effect of Ultrasonic Treatment on the Solidification Microstructure of GCr15 Bearing Steel

Abstract: Ultrasonic treatment with various powers is introduced to liquid steel from the side wall of a mold during GCr15 steel solidification, and the effect of ultrasonic on the microstructure and properties of GCr15 steel is investigated. Results show that the columnar grains in the GCr15 steel are coarse and that the microstructure is inhomogeneous when ultrasonic is not applied on the liquid steel. A suitable power ultrasonic leads to the appearance of a large number of equiaxed grains and increases the uniformity of the microstructure. The segregation of alloy elements gradually decreases as the power increases from 0 W to 500 W. The maximum segregations of carbon and silicon decrease from 2.541 to 1.129 and 2.861 to 1.196, respectively. Given a power of 500 W, the statistical segregations of carbon and silicon decrease from 0.0964 to 0.0693 and 0.1152 to 0.1075, respectively. A further increase in ultrasonic power is not conducive for improving the element segregation. Ultrasonic treatment can remarkably refine the size of carbide and increase the uniformity of its distribution. When the powers are 0 W, 300 W, 500 W, 700 W, and 1,000 W, the average sizes of carbide are 14.63 μm, 2.96 μm, 3.05 μm, 3.72 μm, and 7.83 μm, respectively. The tensile strength, yield strength, and ductility and reduction of the area of the GCr15 bearing steel are correspondingly improved to varying degrees.

Keywords: bearing steel, ultrasonic, element segregation, carbide, mechanical properties

PACS. 64.70.Kd

DOI 10.1515/htmp-2014-0148
Received October 13, 2014; accepted January 21, 2015

***Corresponding author: Jianjun Wang,** School of Metallurgy Engineering, Anhui University of Technology, Ma'anshan 243002, Anhui, China, E-mail: electroslag123@gmail.com
Xiaofang Shi: E-mail: shixiaofang602@163.com, **Lizhong Chang, Haijun Wang:** E-mail: 27713154@qq.com, **Lipeng Meng:** E-mail: 446075894@qq.com, School of Metallurgy Engineering, Anhui University of Technology, Ma'anshan 243002, Anhui, China

Introduction

Rapid developments in machinery, petroleum, chemical, and high-speed railway industries require high-performance steel material. However, an ingot with excellent metallurgical qualities is a precondition to obtaining high-performance steel products.

In order to obtain high metallurgical quality ingots, it is necessary to improve purity, obtain even and compact crystal structures [1–3]. The purity of steel is achieved by reducing gas content and nonmetallic inclusions in steel. Even and compact crystal structures are obtained by reducing or eliminating solidification defects, such as composition segregation, uneven structure, sinkhole, and looseness during liquid metal solidification.

Along with the progress of modern steelmaking processes, particularly the development of secondary refining techniques, the oxygen content, such as of ball bearing steel, can be decreased to < 0.0005%, along with the inclusions. Thus, controlling the purity of steel is not a major limitation in metallurgy production. Continuous casting significantly improves metal yield and production efficiency, but the solidification structure of the billet does not improve despite the application of various advanced technologies, such as tundish heating, electromagnetic stirring, and soft reduction. Therefore, improving the solidification structure of the steel, particularly the solidification structure of high-alloy steel, has increasingly attracted the attention of metallurgists.

In recent years, studies have revealed that the solidification structure of steel can be refined if the liquid steel is given proper ultrasonic treatment during the solidification process [4–7]. However, a key question is: how is ultrasonic introduced into liquid steel? The most common method at present is the direct introduction of ultrasonic into liquid steel via the wave guide rod. However, high-temperature liquid steel can easily erode the wave guide rod, and this method is unsuitable for commercial production. This study investigates the effect of the ultrasonic on the macrostructure of GCr15 bearing steel, composition segregation, refinement and distribution of carbide, and the mechanical properties of steel by introducing the ultrasonic into the liquid steel from the side wall of the mold.

Experimental

Experimental materials

Material used in this research is GCr15 bearing steel and its composition is as follows (wt%): C: 0.96–1.0, Mn: 0.35–0.4, Si: 0.2–0.3, Cr: 1.4–1.5, $P < 0.012\%$, $S < 0.005\%$.

Experimental equipment and analysis instruments

Figure 1 shows the schematic of the ultrasonic treatment apparatus, which consists of some assembled equipment. In this schematic, the JTS-3000 intelligent NC ultrasonic generator V6.0 (no. 1) and the transducer (no. 3) are manufactured by Cheng Gong Ultrasonic Wave Co. Limited, Hangzhou. The wave guide rod (no. 4) is homemade, and the shape of "C," whose radius of curvature is the same as that of the interior radius of the mold, is designed at the point of contact between the wave guide rod and the mold.

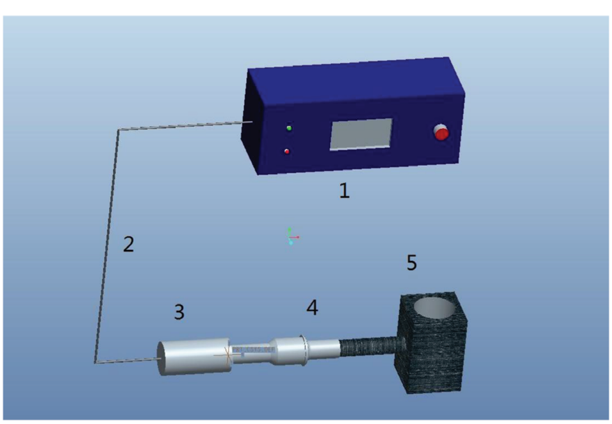

Figure 1: Sketch of ultrasonic experimental equipment.
Notes: 1. Ultrasonic wave generation equipment; 2. wire; 3. ultrasonic transducer; 4. wave guide rod; 5. water-cooled steel mold.

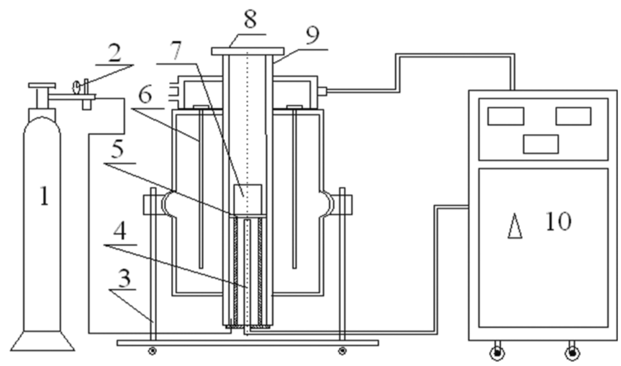

Figure 2: Experimental apparatus of heating equipment.
Notes: 1. Nitrogen; 2. flowmeter; 3. metallic stents; 4. thermocouple; 5. refractory brick; 6. heating material; 7. crucible; 8. furnace cover; 9. furnace tube; 10. control cabinet.

The melting unit is the RKJ-12-16 high-temperature heating furnace, and the heating material is $MoSi_2$, which includes two parts: the gas protection, which is composed of flow meter, control valve, and nitrogen, and the heating furnace, as shown in Figure 2.

The ZEISS-200MAT metallographic microscope is used to observe the solidification structure of steel by ultrasonic treatment with powers of 0 W, 300 W, 500 W, 700 W, and 1,000 W. The mechanical properties of steel are tested using the ZWICK-Z150 electronic stretcher from Germany.

The analytical instrument for element segregation is the original position analysis (OPA) apparatus (NCS Testing Technology Co., Ltd.). OPA can serve various functions, such as segregation, quantity and distribution of inclusion, as well as porosity and chemical composition of steel ingot and is widely used in the metallurgical industry because of its simple sample preparation, accurate quantization, and high-speed analysis compared with conventional analytical methods. The following technical parameters are used for OPA: (1) discharge parameters (continuous excitation system): frequency, 500 Hz; inductance, 120 H; capacitance, 5 F; voltage, 400 V; (2) spectrophotometric system: focal length, 750 mm; spectrum range, 120 nm to 800 nm; distinguishability surpass, 0.01 nm; (3) sample size: length 500 mm × width 245 mm; and (4) load bearing: 20 kg.

Experimental schemes

The experimental schemes employed in this study are shown in Table 1.

Table 1: Experimental schemes.

Schemes	Ultrasonic power, W	Steel	Ultrasonic mode	Applying time, μs	Interval time, ms	Frequency, kHz
1	0	GCr15	Pulse	8,000	2	21
2	300	GCr15	Pulse	8,000	2	21
3	500	GCr15	Pulse	8,000	2	21
4	700	GCr15	Pulse	8,000	2	21
5	1,000	GCr15	Pulse	8,000	2	21

Experimental procedure

The experimental procedure is as follows.

Ultrasonic treatment

The material was placed in a corundum crucible and melted in a heating furnace at a temperature of 1,580°C. The liquid steel was poured into a mold for ultrasonic treatment. The ultrasonic was introduced at room temperature to the molten steel from the side wall of the mold, until the molten steel solidified completely. The powers were 0 W, 300 W, 500 W, 700 W, and 1,000 W, with a frequency of 21 kHz.

Sample preparation

The finished ingots were split lengthwise from the middle and were subsequently polished for use.

Sample analysis

(1) The polished samples were placed in a 50% hydrochloric acid solution and heated in a water bath of 100°C for 2 h. After the erosion, the sample was washed with anhydrous ethanol to observe its macrostructure.

(2) OPA was adopted to quantitatively analyze the segregation of C, Si, Cr, and Mn in the steel ingot. The in situ scanogram spot of the ingot is shown in Figure 3. The line-by-line scan mode was adopted during the sample scanning. The X-axis was used as the continuous scan direction, and the scan speed was 80 mm min^{-1}. The Y-axis was used as the stepping scan, and the stepping spacing was 2 mm.

(3) The sample, which was treated with different powers, was cut into small samples with dimensions of 20 mm × 30 mm, and the distribution of carbide was observed through a metallographic microscope. Tensile samples were machined after forging them at an initial forging temperature of 1,150 °C and a final forging temperature of 850°C. The mechanical properties of the bearing steel were tested. The tensile samples were φ10 mm × 70 mm, and the screw threads were M16 mm × 20 mm.

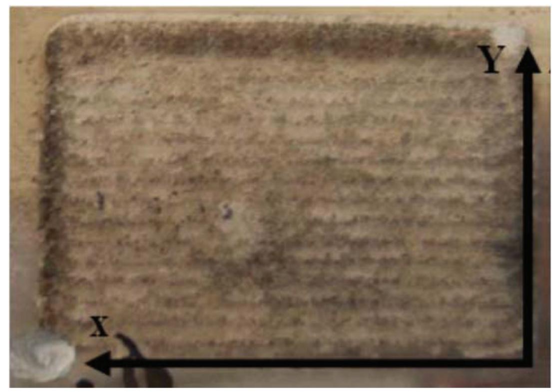

Figure 3: In situ scanogram spot of the steel ingot.

Results and discussion

Influence of ultrasonic on the macrostructure of GCr15 bearing steel

Figure 4 shows the macrostructure of GCr15 steel treated with different powers.

Figure 4 shows that, during the solidification process, the columnar grains of GCr15 steel without ultrasonic are developed and the structure is not uniform. When the power increases to 300 W, the coarse columnar grains are broken, and a large number of equiaxed grains appear, which means that grain refinement is evident and that the structure is uniform. The ratio of equiaxed grains further increases when the power increases to 500 W. When the power increases beyond 500 W, the ratio of equiaxed grains no longer increases.

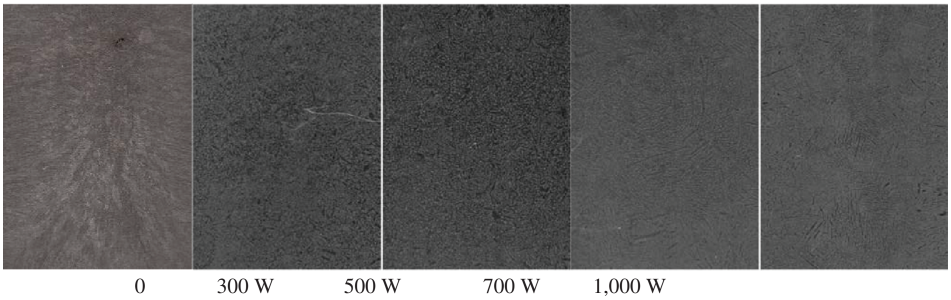

Figure 4: Macrostructure of GCr15 steel treated with different ultrasonic power.

Cavitation and acoustic streaming effects are produced during the solidification process of liquid steel when the ultrasonic is introduced. When the wave spreads through the media, resonance occurs between the wave and tiny bubbles in the media. When the ultrasonic reaches a certain value, the pressure inside the bubbles becomes lower than the original pressure. The bubble expands quickly at the sparse part of the wave trough, but compresses abruptly, explodes, and then disappears at the dense part of the wave peak. The "formation–development–explosion" process of small bubbles constitutes the ultrasonic cavitation effect. The ultrasonic forms cavitation bubbles in the liquid steel, thereby reducing the temperature on the surface of the cavitation bubbles and facilitating the formation of the nucleus around the bubbles in the molten steel. Some solid particles in the liquid steel have surface defects because of the ultrasonic cavitation effect, and the weak particles may break into smaller ones and be distributed evenly in the liquid steel under the actions of ultrasonic acoustic streaming, heat flow, and cavitation effect. Similarly, the dendrite in the mushy zone is broken into pieces. Hence, the ratio of the columnar grains of the steel decreases, whereas the ratio of equiaxed grains increases [8–11].

The experimental results show that, if the ultrasonic power is too high or too low, the effect on the refinement of the solidification structure is not obvious. The power has a threshold value; when the power is lower than this threshold, the ultrasonic treatment can noticeably improve the solidification structure with an increase of power. However, when the power is beyond this threshold, the influence is not so obvious. In this experimental condition, the best effect occurs when the power is between 300 W and 500 W.

Influence of ultrasonic on composition segregation of GCr15 steel

Figure 5 shows the variations in carbon, silicon, manganese, and chromium segregations as a function of the power, which is assessed through the statistical and maximum segregations of the elements.

The statistical segregation is calculated according to the formula

$$S = \sigma / C_0$$
$$\sigma = \left[\sum (C - C_0)^2 / N\right]^{1/2} \tag{1}$$

where C_0 represents the average element content, C represents the element contents at different positions, N represents the collected spot number; σ represents confidence expansion range of C_0 at 95 % confidence level and 95 % confidence interval is between $(C_0 - \sigma)$ and $(C_0 + \sigma)$. The larger is the statistical segregation, more serious is the segregation, but rather the contrary. The statistical segregation is zero if there is no segregation.

The maximum segregation is calculated according to the formula

$$X = \frac{C_{\max}}{C_0} \tag{2}$$

where C_0 represents the average element content and $C_{\max}$ represents the maximum element content on the longitudinal section of steel ingot.

Figure 5 shows that, when no ultrasonic is introduced during the solidification process of GCr15 steel, the statistical segregations of carbon and silicon are 0.0964 and 0.1152 and the maximum segregations are 2.541 and 2.861, respectively. When the ultrasonic power increases to 300 W, the statistical segregations and maximum segregation of carbon and silicon decrease to 0.0706, 0.1101 and 1.163, 1.445, respectively. By contrast, the statistical and maximum segregations of manganese and chromium increase slightly. When the power increases to 500 W, the statistical and maximum segregations of all the elements decrease, which shows that the ultrasonic effectively restrains the segregation of the elements in the solidification process. This occurrence may be attributed to the refinement of the solidification microstructure by the ultrasonic, which reduces the formation

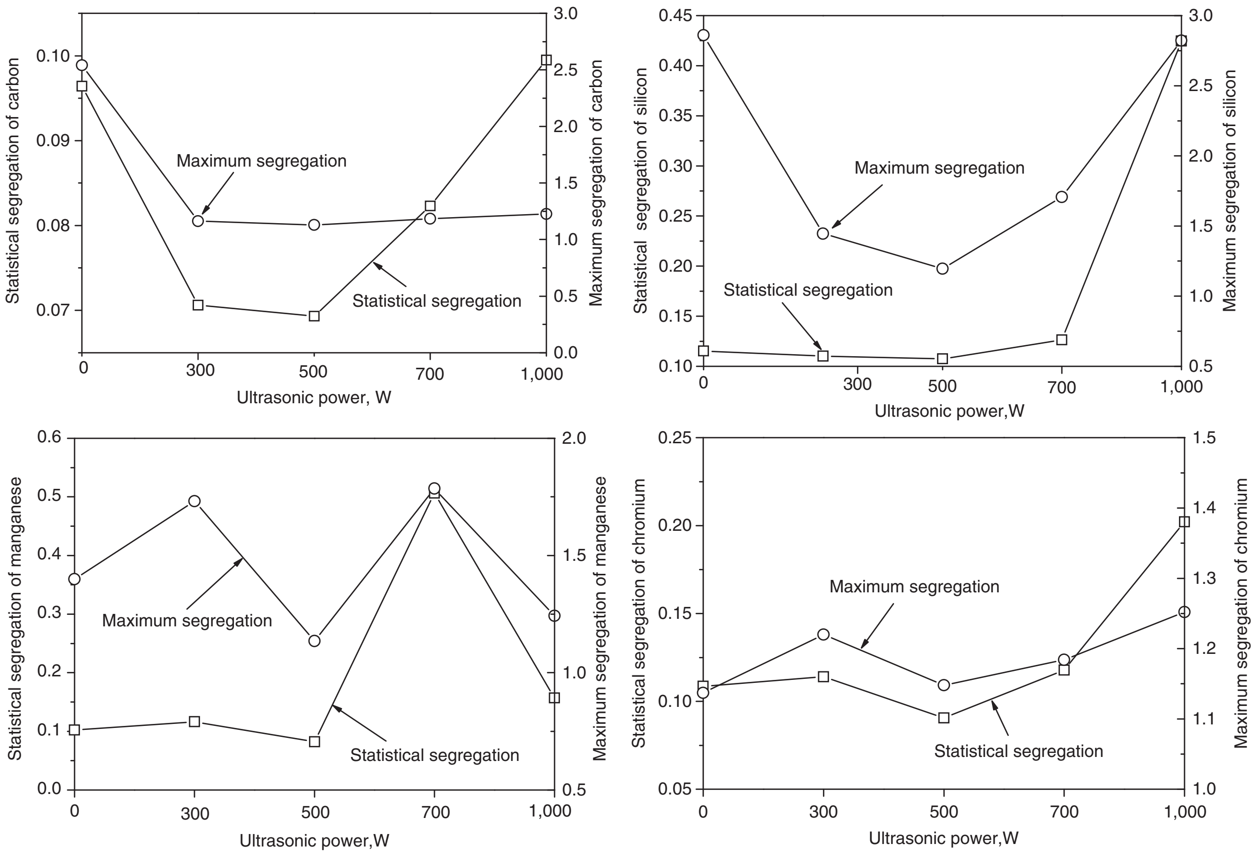

Figure 5: Relation between the segregation and ultrasonic power.

of columnar grains and leads to the uniform distribution of the alloy elements in the liquid steel as a result of the ultrasonic cavitation and acoustic streaming effects.

However, when the power further increases to 700 W and 1,000 W, the segregation increases instead. Excessive ultrasonic power initiates the violent motion of the molten steel, thereby removing the enriched steel surrounding the dendrites in the mushy zone and reducing the solute content in the region. As a result, severe element segregation occurs.

Influence of ultrasonic treatment on carbide and mechanical properties of GCr15 steel

Given that a bearing has to endure high impact and alternating load, the size and distribution of carbide must be controlled for good macro- and micro-structures, and the fatigue life and wear-resisting property must be guaranteed. With a sharp or rough surface for large carbide particles, stress concentration tends to form at the point of contact between the carbide and matrix, thereby shortening the service life of the ball bearing steel. Stress concentration does not easily form when the carbide particles are small and spherical in shape [13]. Figure 6 shows the average diameter and area percentage of carbide in GCr15 steel subjected to ultrasonic treatment with different powers. To facilitate the statistics of carbide in steel, the carbide is assumed to be $(FeMe)_3C$ [12, 14, 15].

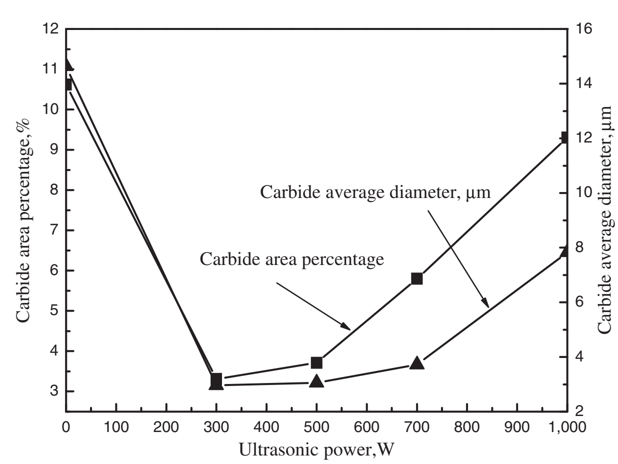

Figure 6: Relation between area percentage, average diameter of the carbide, and ultrasonic power.

Prior to ultrasonic treatment, the area of the carbide accounts for 10.62% of the field of view, and its average size is 14.63 μm. When the powers are 300 W, 500 W, 700 W, and 1,000 W, the area of the carbide accounts for 3.31%, 3.71%, 5.80%, and 9.30%, and its average sizes are 2.96 μm, 3.05 μm, 3.72 μm, and 7.83 μm, respectively. Small carbide particles do not easily form a stress concentration, but their concentrated distribution may lead to stress concentration [14]. Therefore, the distribution and size of carbide have a significant influence on the properties of bearing steel, particularly fatigue life and toughness. The size of carbide must consequently be refined and the uniformity of its distribution be increased to improve the property of the ball bearing steel.

The metallograph for the distribution of carbide is shown in Figure 7(A). The metallographs are processed, as shown in Figures 7(B) and 8, to clearly observe the carbides in the steel. The white particles in Figure 7(B) are the carbides.

Figure 8(A) shows the distribution of carbide before the introduction of the ultrasonic to the liquid steel. Figure 8(A) shows that the carbides have a mesh distribution and that the largest size in the statistical field of view is 14.63 μm. After introducing the ultrasonic, both

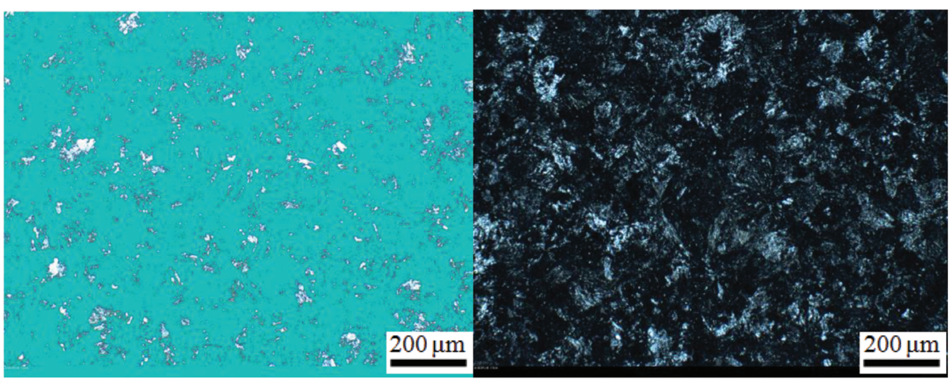

Figure 7: Carbide distribution before (A) and after (B) the image processing (the ultrasonic power of 500 W).

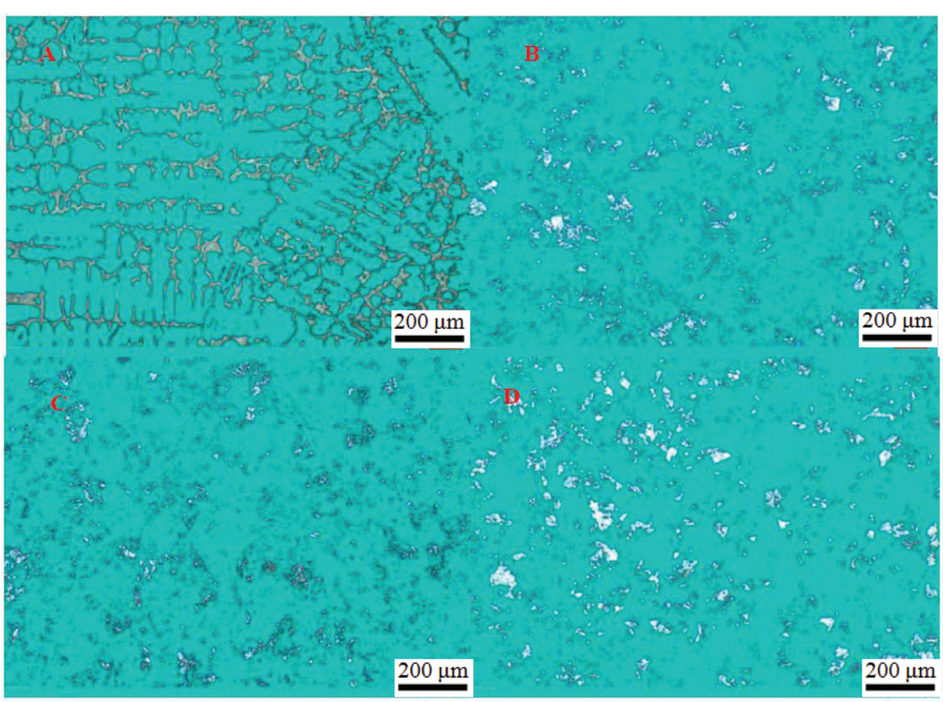

Figure 8: Carbide distribution of GCr15 steel with different ultrasonic power.

the distribution and size of carbide improve noticeably. Many nonlinear effects, such as acoustic steaming and cavitation effects, produced by the ultrasonic in the liquid steel can disintegrate the dendritic crystals and carbide in the solidification process. Thus, the carbide particles are refined, and the uniformity of their distribution is increased. Figure 8(B) shows that, after treatment with 300 W ultrasonic power, the distribution of carbide becomes uniform and the mesh disappears, while large amounts of small and round carbide particles appear, thereby improving the property of the bearing steel. Figure 7(B) shows the distribution of carbide treated with 500 W ultrasonic power. The carbide distribution is uniform, and its size is similar to the carbides in Figure 8 (B). After introducing 700 W and 1,000 W ultrasonic powers, the distribution of carbide remains almost unchanged, and its size increases (Figure 8(C) and (D)). The above analysis reveals that, when the power increases from 0 W to 500 W, the size of carbide decreases. However, the size increases as the power increases further.

To further confirm the favorable influence of ultrasonic treatment on the solidification microstructure, the mechanical properties of GCr15 steel are tested. First, the steel ingot treated with the ultrasonic is forged and annealed. The changes in its tensile strength, yield strength, ductility, and reduction of its area are tested. After the ultrasonic treatment, its tensile strength, yield strength, ductility, and reduction of its area improve, as shown in Figure 9. When the power is 300 W, its tensile strength, yield strength, ductility, and reduction of its area improve to a maximum of 653 MPa, 370 MPa, 58%, and 27%, respectively. The mechanical property indexes worsen as the ultrasonic power increases further, which is in accordance with that shown in Figure 8. The smaller the size of the carbide, the more uniform its distribution, and the better its mechanical properties at room temperature.

Conclusions

(1) Introducing the ultrasonic from the side wall of the mold into the solidification process of GCr15 steel evidently refines the solidification structure, decreases the ratio of columnar grains, and increases the ratio of equiaxed grains. In this experimental condition, the best effect is achieved when the ultrasonic power is between 300 W and 500 W.

(2) When the ultrasonic power increases to 300 W, the statistical and maximum segregations of carbon and silicon decrease. The statistical and maximum segregations of all the elements improve when the ultrasonic power increases to 500 W. Excessive ultrasonic power increases the segregation of the element.

(3) Ultrasonic treatment can remarkably refine the size of carbide and increase the uniformity of its distribution. When the ultrasonic powers are 0 W, 300 W, 500 W, 700 W, and 1,000 W, the average sizes of carbide are 14.63 μm, 2.96 μm, 3.05 μm, 3.72 μm, and 7.83 μm, respectively. Corresponding to these results, the tensile strength, yield strength, ductility, and reduction of the area of GCr15 bearing steel improve to varying degrees.

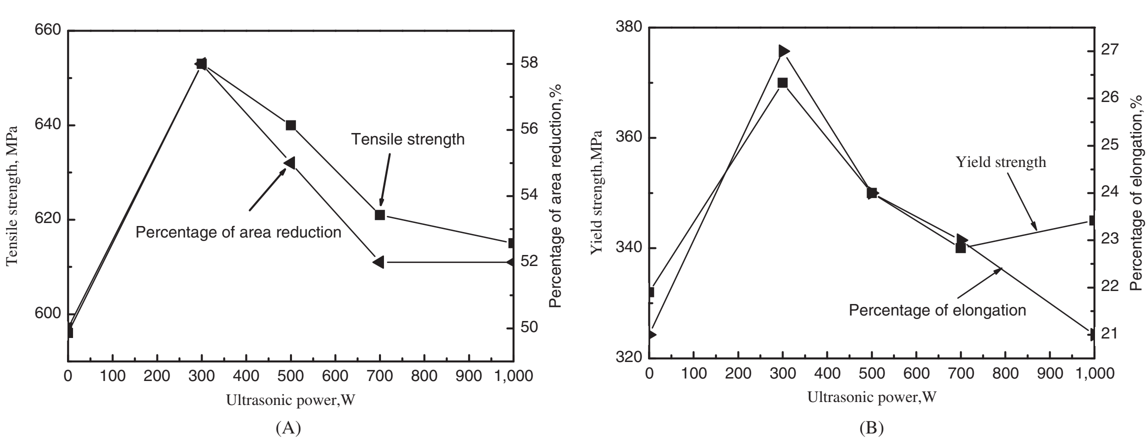

Figure 9: Mechanical properties of GCr15 steel with different ultrasonic power. (A) Tensile strength and reduction of area after ultrasonic treatment. (B) Yield strength and percentage of elongation after ultrasonic treatment.

Acknowledgment: The authors would like to express their gratitude to the National Natural Science Foundation of China for financial support (Grant No. 51274004/51104001).

References

[1] Kaushik P, Lowry M, Yin H. Inclusion characterisation for clean steelmaking and quality control. Ironmaking Steelmaking 2012;39:284–300.
[2] Gao S, Zhai Q, Qi F, Fu Z-y, Gong Y-y. Application and development of high-intensity ultrasonic in solidification process of metals. Mater Rev 2002;16:5–6.
[3] Kang YJ, Yu L, Sichen D. Study of inclusion removal mechanism around open eye in ladle treatment. Ironmaking Steelmaking 2007;34:253–61.
[4] Das A, Kotadia HR. Effect of high-intensity ultrasonic irradiation on the modification of solidification microstructure in a Si-rich hypoeutectic Al-Si alloy. Mater Chem Phys 2011;125:853–9.
[5] Liu X, Osawa Y, Takamori S, Mukai T. Microstructure and mechanical properties of AZ91 alloy produced with ultrasonic vibration. Mater Sci Eng A 2008;487:120–3.
[6] Zhang S, Zhao Y, Cheng X, Chen G, Dai Q. High-energy ultrasonic field effects on the microstructure and mechanical behaviors of A356 alloy. J Alloys Compd 2009;470:168–72.
[7] Han Y, Li K, Wang J, Shu D, Sun B. Influence of high-intensity ultrasound on grain refining performance of Al–5Ti–1B master alloy on aluminium. Mater Sci Eng A 2005;405:306–12.
[8] Wang J-j, Li Q, Zhou L, Jin Y-l, Chang L-z. Optimization study of molten steel solidification structure under ultrasonic treatment. Chin J Process Eng 2006;6:53–6.
[9] Liu QM, Zhai QJ, Qi FP, Zhang Y. Effects of power ultrasonic treatment on microstructure and mechanical properties of T10 steel. Mater Lett 2007;61:2422–5.
[10] Li J, Chen W-q, He B-X, Wang X-f, Liu Q. Effect of different ultrasonic treatments on solidification structure of high carbon liquid steel. Fundry 2007;56:754–6.
[11] Liu Q-m, Gong Y-y, Hou X, Qi F-p, Zhai Q-j. Influence of side ultrasonic treatment on solidification characterization of Al-Si eutectic alloy. Chin J Nonferrous Metals 2007;17:308–12.
[12] Li W, Liu ZM. Research about carbide high-temperature diffusion of GCr15 bearing steel. He Bei Metall 2012;3:23–5.
[13] Baoping F, Yajun Q, Chuanen W, Yali M, Linxia L. Effect of carbide on of fatigue life of GCr15 bearing steel. Bearing 2003;10:30–2.
[14] Zhongqi D, Min C, Rui C, Di Y, Zhenmin L. Influence of high temperature diffusing process on carbide precipitation of GCr15 bearing steel. Bearing 2011;7:25–8.
[15] Wang J, Chat F. Effect of carbide refinement on the fine structure of bainite/martensite duplex microstructure of GCr15 steel. J Mater Sci Lett 1994;13:1506–9.